provide a fourth coordination interaction for the bridging irons. It is quite clear from these maps that no sulfur is present in the center of the cluster.

Functionally, the details of the interaction between N_2 and the FeMo-cofactor are central to the understanding of the catalytic properties of nitrogenase. Although many models can be envisioned for the binding of substrates to the FeMo-cofactor on the basis of the Kim structural model, an intriguing hypothesis can be developed for the coordination mode of N_2 to the cofactor that would facilitate triple-bond cleavage. The FeMo-cofactor contains three weak Fe–Fe bonds that are further destabilized by the distortion from idealized tetrahedral geometry. Thus, it is tempting to suggest that N_2 could bind in the center of the FeMo-cofactor, thereby replacing the weak Fe–Fe bonds with multiple Fe–N bonds having approximate sp^3 geometry (Fig. 3). As a result of these multiple Fe-N interactions, the *sp* hybridized N≡N triple bond should be weakened, thereby lowering the activation barrier for N_2 reduction. Features of this model of N_2 coordination have been observed for nitrogen analogs binding to trinuclear and dinuclear metal clusters (*11*). Although the cavity size in the FeMo-cofactor structure is too small by ~0.5 Å for N_2 to fit in this fashion, the more reduced forms of the cofactor that are believed to actually bind N_2 (*12*) may have an increased separation distance between bridged Fe-Fe sites that could accommodate N_2 binding. Unlike most substrates and intermediates, however, only N_2 is potentially small enough to coordinate inside the FeMo-cofactor, suggesting that alternative binding modes may be utilized by different substrates, reaction intermediates, and inhibitors. This model for the binding of the N_2 to the FeMo-cofactor may be useful for the understanding of the mechanistic steps associated with N_2 reduction by nitrogenase, and it could guide the development of other hosts and catalysts that can specifically interact with N_2.

REFERENCES AND NOTES

1. B. K. Burgess, in *Advances in Nitrogen Fixation Research*, C. Veeger and W. E. Newton, Eds. (Nijhoff, Boston, 1984), pp. 103–114; ,W. H. Orme-Johnson, *Annu. Rev. Biophys. Biophys. Chem.* **14**, 419 (1985); R. H. Holm and E. D. Simhon, in *Molybdenum Enzymes*, T. G. Spiro, Ed. (Wiley, New York, 1985), chap. 2; E. I. Steifel *et al.*, *Am. Chem. Soc. Symp. Ser.* **372**, 372 (1988); R. H. Burris, *J. Biol. Chem.* **266**, 9339 (1991); B. E. Smith and R. R. Eady, *Eur. J. Biochem.* **205**, 1 (1992).
2. J. Kim and D. C. Rees, *Science* **257**, 1677 (1992).
3. W. H. Orme-Johnson, *ibid.*, p. 1639; A. S. Moffat, *ibid.*, p. 1624.
4. CCP4; The SERC (U.K.) Collaborative Computing Project No. 4, A Suite of Programs for Protein Crystallography, distributed from Daresbury Laboratory, Warrington WA4 4AD, United Kingdom.
5. A. T. Brunger, *J. Mol. Biol.* **203**, 803 (1988).
6. D. E. Tronrud, L. F. Ten Eyck, B. W. Matthews, *Acta Crystallogr. Sect. A* **43**, 489 (1987).
7. J. Kim and D. C. Rees, *Nature* **360**, 553 (1992).
8. K. S. Bose, E. Sinn, B. A. Averill, *Organometallics* **3**, 1126 (1984).
9. D. Seyferth, A. M. Kiwan, E. Sinn, *J. Organomet. Chem.* **281**, 111 (1985); H. L. Blonk *et al.*, *Inorg. Chem.* **31**, 962 (1992).
10. M. K. Chan, J. Kim, D. C. Rees, unpublished data.
11. P. E. Baikie and O. S. Mills, *J. Chem. Soc. Chem. Commun.* **1967**, 1228 (1967); C. T.-W. Chu, R. S. Gall, L. F. Dahl, *J. Am. Chem. Soc.* **104**, 737 (1982); D. Sellmann, P. Kreutzer, G. Huttner, A. Frank, *Z. Naturforsch. Teil B* **33**, 1341 (1978); D. Sellmann, W. Soglowek, F. Knoch, M. Moll, *Angew. Chem. Int. Ed. Engl.* **28**, 1271 (1989); G. D. Williams, G. L. Geoffroy, R. R. Whittle, A. L. Rheingold, *J. Am. Chem. Soc.* **107**, 729 (1985); F. A. Cotton, B. E. Hanson, J. D. Jamerson, B. R. Stults, *ibid.* **99**, 3293 (1977); M. D. Brice and B. R. Penfold, *Inorg. Chem.* **11**, 1381 (1972).
12. R. N. F. Thorneley and D. J. Lowe, in *Molybdenum Enzymes*, T. G. Spiro, Ed. (Wiley, New York, 1985), pp. 221–284.

13. Discussions with J. E. Bercaw and J. B. Howard and the assistance of J. Schlessman, T. McPhillips, M. Stowell, A. Chirino, D. Woo, B. T. Hsu, and D. Malerba are appreciated. Research supported by NSF grant DMB 91-18689. M.K.C. is the recipient of NIH fellowship 1F32 GM15006. The rotation camera facility at the Stanford Synchrotron Radiation Laboratory is supported by the Department of Energy, Office of Basic Energy Sciences, and the NIH Biomedical Resource Technology Program, Division of Research Resources. The program X-PLOR was run on the CRAY-YMP at the San Diego Supercomputer Center, supported by NSF.

13 October 1992; accepted 28 January 1993

The Ischigualasto Tetrapod Assemblage (Late Triassic, Argentina) and $^{40}Ar/^{39}Ar$ Dating of Dinosaur Origins

Raymond R. Rogers, Carl C. Swisher III, Paul C. Sereno, Alfredo M. Monetta, Catherine A. Forster, Ricardo N. Martínez

$^{40}Ar/^{39}Ar$ dating of sanidine from a bentonite interbedded in the Ischigualasto Formation of northwestern Argentina yielded a plateau age of 227.8 ± 0.3 million years ago. This middle Carnian age is a direct calibration of the Ischigualasto tetrapod assemblage, which includes some of the best known early dinosaurs. This age shifts last appearances of Ischigualasto taxa back into the middle Carnian, diminishing the magnitude of the proposed late Carnian tetrapod extinction event. By 228 million years ago, the major dinosaurian lineages were established, and theropods were already important constituents of the carnivorous tetrapod guild in the Ischigualasto–Villa Unión Basin. Dinosaurs as a whole remained minor components of tetrapod faunas for at least another 10 million years.

Dinosaurs originated sometime during the Middle to Late Triassic and rose to dominate terrestrial tetrapod communities by the end of the Triassic. The earliest skeletal records of dinosaurs are preserved in Carnian age strata on several continents, including North America (Chinle Group), South America (Ischigualasto and Santa Maria formations), India (Maleri Formation), and Africa (Timesgadiouine Formation) (*1*, *2*). The most complete skeletons of early dinosaurs, discovered in the Ischigualasto Formation of Argentina, include the primitive theropods *Herrerasaurus* and *Eoraptor* (*3*) and the primitive ornithischian *Pisanosaurus* (*4*). These genera, along with *Staurikosaurus* from the Santa Maria Formation of Brazil, have long been considered the oldest dinosaurs (*5*, *6*). Recently, all of these early dinosaur localities were assigned a late Carnian (Tuvalian) age on the basis of biostratigraphic correlations, which suggests that dinosaurs appeared nearly simultaneously across most of Pangea (*7*).

In this report, we present radioisotopic age data from the Ischigualasto Formation and describe the stratigraphic ranges and abundances of Ischigualasto dinosaurs relative to other tetrapods in the paleofauna. These data calibrate the first appearance of dinosaurs and permit a more rigorous evaluation of major extinction and origination events during the Late Triassic (*8*, *9*).

The Ischigualasto Formation is part of the Agua de la Peña Group, a succession of nonmarine Triassic rocks exposed in the Ischigualasto–Villa Unión Basin of northwestern Argentina (Fig. 1). This basin is one of several small rift basins that formed along the western margin of South America before the breakup of Pangea (*10*). The Ischigualasto Formation is composed of fluvial sandstone bodies and fine-grained overbank facies. Deposition occurred on an upland alluvial plain characterized by low sinuosity, shallow streams, occasional lakes, and a seasonal climate (*11*).

R. R. Rogers, Department of Geophysical Sciences, University of Chicago, Chicago, IL 60637.
C. C. Swisher III, Geochronology Center, Institute of Human Origins, Berkeley, CA 94709.
P. C. Sereno and C. A. Forster, Department of Organismal Biology and Anatomy, University of Chicago, Chicago, IL 60637.
A. M. Monetta and R. N. Martínez, Museo de Ciencias Naturales, Universidad Nacional de San Juan, San Juan 5400, Argentina.

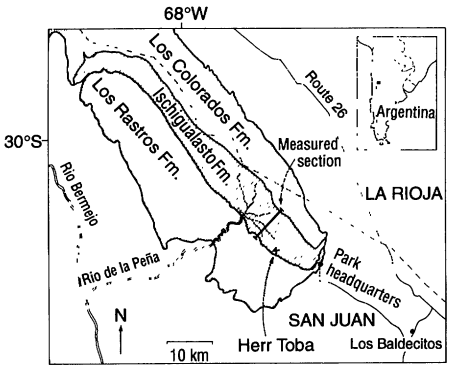

Fig. 1. Location of Ischigualasto–Villa Unión Basin in San Juan and La Rioja provinces, northwestern Argentina (inset). This basin preserves an almost 4000-m-thick succession of Triassic nonmarine strata (*15*) that includes the Ischigualasto Formation and other important tetrapod-bearing units (the overlying Los Colorados Formation and the Chañares Formation). We focused near the southern end of the basin in the Valle de la Luna region of Ischigualasto Provincial Park (the section we measured and the location of the Herr Toba bentonite are marked).

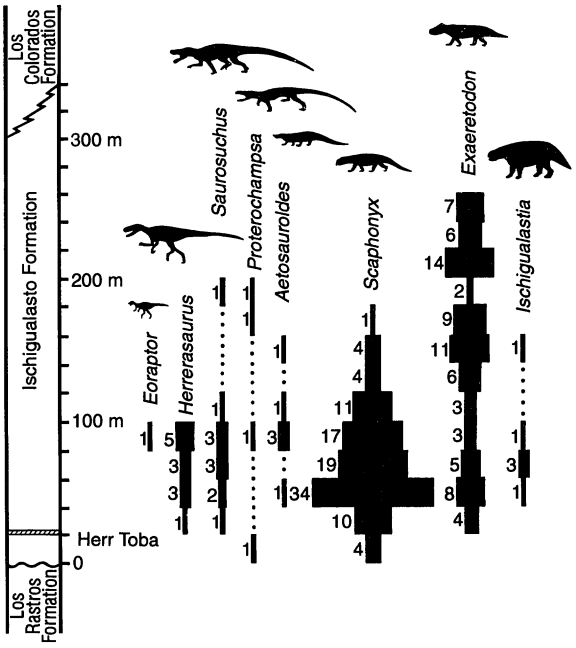

Fig. 2. Range chart illustrating the stratigraphic distributions (vertical axis is elevation in meters above the Los Rastros Formation) and relative abundances of eight major Ischigualasto taxa. The position of the Herr Toba bentonite is also indicated. Taxa include the dinosaurs *Eoraptor* and *Herrerasaurus*, the rauisuchian *Saurosuchus*, the proterochampsid *Proterochampsa*, the aetosaur *Aetosauroides*, the rhynchosaur *Scaphonyx*, the traversodont cynodont *Exaeretodon*, and the dicynodont *Ischigualastia*. The sampling interval is 20 m. Specimen abundance at each interval is indicated numerically and is also scaled to the width of the bars. Each of the 228 tetrapod specimens recorded represents one individual (*29*). Not included in this diagram are two specimens of amphibians (140 to 160 m and 200 to 220 m), a specimen of *Trialestes* (140 to 160 m), and six undescribed specimens of carnivorous cynodonts (40 to 100 m, 240 to 260 m, and 280 to 300 m). All specimens in the diagram were mapped in 1988 and 1991, except for the highest *Proterochampsa* (MCZ 3408) and *Saurosuchus* (PVL 2062) (*30*). MCZ, Museum of Comparative Zoology, Harvard University; PVL, Instituto Miguel Lillo, Tucumán, Argentina.

Tetrapods of the Ischigualasto paleofauna include primitive dinosaurs (*Herrerasaurus*, *Eoraptor*, and *Pisanosaurus*), nondinosaurian archosaurs, herbivorous and carnivorous cynodonts, dicynodonts, rhynchosaurs, and temnospondyl amphibians. We found 228 tetrapod fossils representing eight genera in the Valle de la Luna region of Ischigualasto Provincial Park (Fig. 1) (*12*). Stratigraphic ranges for these genera were determined by direct correlation of the specimens to a local stratigraphic section spanning the formation (Fig. 2).

Most Ischigualasto tetrapods occur in the lower two-thirds of the formation, where the rhynchosaur *Scaphonyx* and the cynodont *Exaeretodon* are most abundant (Fig. 2). The decrease in abundance and eventual loss of *Scaphonyx* in the upper part of the section appear to represent a true local extinction. The fossils of *Exaeretodon*, which occur in the same facies as those of *Scaphonyx* but extend much higher in the section, provide taphonomic control (*13*) to support this interpretation. A correlation has been proposed between the extinction of the rhynchosaurs and the demise of the *Dicroidium* flora (*14*); however, fossil plants of *Dicroidium* affinity occur throughout the Ischigualasto Formation and are also present in the overlying Los Colorados Formation (*15*).

Among dinosaurs, *Herrerasaurus* is most abundant and appears to be restricted to the lower third of the formation (Fig. 2). The single specimen of *Pisanosaurus* was collected from the middle third of the formation (*4*, *16*). Dinosaur specimens comprise only 5.9% of the total tetrapod sample but account for 37% of all terrestrial carnivores. If small-bodied carnivores (cynodonts) are excluded, dinosaurs comprise approximately 45% of the carnivore sample (*17*). The scarcity of fossils in the upper third of the Ischigualasto Formation remains enigmatic, as neither sedimentary facies nor preservational styles (*18*) differ significantly from those that characterize the lower part of the section.

The age of the Ischigualasto tetrapod assemblage was determined by $^{40}Ar/^{39}Ar$ incremental laser heating of fine-grained sanidine crystals extracted from a bentonite (Herr Toba site) that intersects the ranges of most Ischigualasto taxa (Fig. 2) (*19*). Two $^{40}Ar/^{39}Ar$ incremental heating analyses of the Herr Toba sanidine (Table 1) yielded well-defined spectra (Fig. 3). The plateau ages were calculated as the weighted (by inverse variances) mean of all increments defining the plateau. Both of the spectra are essentially flat; the plateaus consist of more than three contiguous increments that overlap the mean at the 2σ level and include over 90% of the total ^{39}Ar released (*20*). Approximately 75% of the total ^{39}Ar was released in the last three increments of highest temperature as a result of a coupling effect of the Ar-ion laser with the sanidine crystals. The plateau ages for the two spectra [228.06 ± 0.78 million years ago (Ma) and 227.78 ± 0.30 Ma (SE)] are virtually identical. A slightly revised heating schedule for the second analysis resulted in a much refined spectrum; we consider it to be the best estimate of the age of the Herr Toba bentonite.

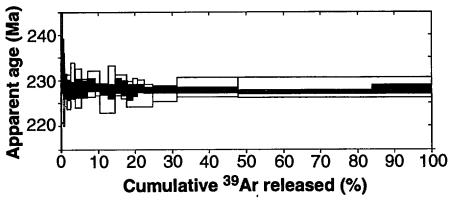

Fig. 3. Incremental heating spectra ($^{40}Ar/^{39}Ar$) for the Herr Toba bentonite. Sample 6260-01, open; sample 6260-02, solid (*31*).

The Herr Toba bentonite is only 20 m above the base of the Ischigualasto Formation (Fig. 2), indicating that deposition of the formation began approximately 228 Ma, during the middle Carnian (*21*). Although the age of the upper boundary of the formation remains unconstrained, sedimentation rates in comparable rift-basin settings (*22*) suggest that the 340-m-thick Ischigualasto section would have accumulated rapidly, probably in 1 to 4 million years (85 to 340 m per million years). Hence, the Carnian-Norian boundary, which has been placed arbitrarily between the Ischigualasto and Los Colorados formations (*15*, *23*), probably occurs within the Los Colorados Formation. The Ischigualasto paleofauna, which is essentially restricted to the lower two-thirds of the Ischigualasto section, is most likely middle Carnian in age.

In consideration of this middle Carnian

Table 1. Incremental heating analyses ($^{40}Ar/^{39}Ar$) of sanidine from the Herr Toba bentonite (*19*).

Sample step	^{39}Ar (%)	$^{37}Ar/^{39}Ar$	$^{36}Ar/^{39}Ar$	$^{40}Ar^*/^{39}Ar$	$^{40}Ar^*$ (%)	Age (Ma)	
						Mean	1σ
			Sample 6260-01				
A	0.01	0.01195	0.05836	4.39076	20.3	87.28	117.93
B	0.19	0.03834	0.03718	5.40057	32.9	106.78	12.39
C	0.32	0.02668	0.00493	8.57073	85.3	166.64	4.64
D	0.39	0.01517	0.00112	11.97466	97.2	228.77	4.04
E	0.55	0.00852	0.00080	11.92174	97.9	227.82	3.88
F	0.65	0.00759	0.00023	11.92592	99.3	227.89	1.73
G	0.88	0.00771	0.00021	11.89602	99.3	227.36	1.84
H	1.03	0.00624	0.00029	12.03504	99.1	229.85	1.87
I	3.47	0.00662	0.00015	11.94074	99.5	228.16	1.08
J	3.48	0.00713	0.00001	12.03424	99.8	229.84	1.10
K	3.91	0.00664	−0.00001	11.82814	99.9	226.14	1.50
L	2.96	0.00662	0.00008	11.97425	99.6	228.76	1.10
M	6.87	0.00701	0.00007	11.85427	99.7	226.61	1.23
N	6.81	0.00710	0.00018	11.87683	99.4	227.02	0.86
O	16.26	0.00708	0.00019	11.96594	99.4	228.61	1.10
P	52.20	0.00708	0.00008	11.95942	99.6	228.50	1.16
			Sample 6260-02				
A	0.00	0.27981	0.20737	−32.56149	−113.4	−826.78	691.58
B	0.01	0.00000	0.25549	5.99131	7.4	118.09	293.83
C	0.02	0.00000	0.02346	9.38026	57.4	181.61	57.07
D	0.08	0.03278	0.01336	9.37912	70.3	181.59	12.44
F	0.21	0.02703	0.00258	12.40402	94.1	236.46	4.64
G	0.51	0.01104	0.00155	12.34105	96.3	235.33	1.97
H	0.77	0.01252	0.00111	11.96762	97.2	228.65	1.32
I	1.00	0.00954	0.00030	11.93005	99.1	227.97	1.15
J	1.19	0.00517	0.00002	11.92798	99.8	227.93	0.88
K	1.66	0.00460	0.00006	11.95078	99.7	228.34	2.13
L	1.68	0.00508	0.00011	11.93568	99.6	228.07	0.96
M	1.86	0.00626	0.00001	11.95100	99.8	228.35	1.08
N	1.85	0.00662	0.00017	11.92957	99.4	227.96	0.72
O	1.83	0.00689	0.00010	11.93513	99.6	228.06	0.71
P	1.76	0.00566	0.00012	12.02337	99.5	229.65	1.82
Q	1.75	0.00404	0.00008	11.97526	99.6	228.78	0.84
R	1.53	0.00789	0.00023	11.92756	99.3	227.93	1.02
S	1.54	0.00639	0.00024	11.91851	99.2	227.76	1.06
T	1.38	0.00652	0.00030	11.95432	99.1	228.41	1.03
U	1.68	0.00732	0.00015	11.97343	99.5	228.75	0.77
V	25.18	0.00788	0.00002	11.94464	99.8	228.23	0.52
W	36.34	0.00728	0.00010	11.97156	99.6	228.72	0.77
X	16.18	0.00709	0.00010	11.93248	99.6	228.01	0.54

*Radiogenic.

age, there are two possibilities regarding the first appearance of the dinosaurs: (i) the Ischigualasto dinosaurs (*Herrerasaurus*, *Eoraptor*, and *Pisanosaurus*) are the oldest known dinosaurs, and dinosaurs do not appear in the fossil record simultaneously or (ii) all early dinosaur localities currently correlated with the Ischigualasto tetrapod assemblage are also middle Carnian in age. We know of no taphonomic reason to suspect a nearly synchronous global first appearance of dinosaurs. However, more radioisotopic dating is required before temporal relationships can be fully resolved.

The age, relative abundance, and range data also bring evidence to bear on the proposed late Carnian tetrapod extinction event (*8*). The Ischigualasto tetrapod assemblage has been used in conjunction with other paleofaunas of presumed late Carnian age to support a mass extinction among tetrapods at the end of the Carnian Age. A shift of the Ischigualasto paleofauna further back into the Carnian, away from the Carnian-Norian boundary, brings the magnitude of this event into question by reducing the number of last appearance events known in the late Carnian (*24*). Recent discoveries in the Chinle Formation of Arizona further indicate that herrerasaurids range into the Norian (*25*) and can no longer be used to support an end Carnian event.

The Ischigualasto tetrapod record has also been cited as an example of competitive replacement (*9*) in which the decline of the therapsids (cynodonts and dicynodonts) is attributed to competitive pressure from contemporary archosaurs and rhynchosaurs (*16*). This notion is not supported by our data on relative abundances and ranges (Fig. 2). Theropod dinosaurs (*Herrerasaurus* and *Eoraptor*) occur in the same facies as other archosaurian (*Saurosuchus* and *Proterochampsa*) and cynodont carnivores, but inverse trends in species richness and relative abundance are not evident. Similarly, inverse trends in the abundances of *Scaphonyx* and *Exaeretodon* are lacking, and *Exaeretodon* persisted within the Ischigualasto–Villa Unión Basin while *Scaphonyx* became locally extinct.

Together, the age and abundance data indicate that, by 228 Ma, the major dinosaurian lineages (Ornithischia, Sauropodomorpha, and Theropoda) were established. Thus, the initial dinosaurian radiation occurred before the middle Carnian. By 228 Ma, theropods were already important constituents of the carnivorous tetrapod guild (*26*) within the Ischigualasto–Villa Unión Basin. Plant-eating ornithischians and sauropodomorphs, on the other hand, were apparently rare components of the herbivorous tetrapod community. Despite the early appearance of key dinosaurian adaptations, such as tooth-to-tooth slicing among dinosaurian herbivores (*27*) and manual grasping and other modifications among dinosaurian predators (*3*), dinosaurs as a whole remained relatively minor components of Late Triassic tetrapod faunas for at least 10 million years.

REFERENCES AND NOTES

1. R. H. Brown, *Am. Assoc. Pet. Geol. Bull.* **64**, 988 (1980).
2. D. B. Weishampel, in *The Dinosauria*, D. B. Weishampel, P. Dodson, H. Osmólska, Eds. (Univ. of California Press, Berkeley, 1990), pp. 63–139.
3. P. C. Sereno, *J. Vertebr. Paleontol.*, in press; _____ and F. E. Novas, *ibid.*, in press; *Science* **258**, 1137 (1992); P. C. Sereno, C. A. Forster, R. R. Rogers, A. M. Monetta, *Nature* **361**, 64 (1993).
4. J. F. Bonaparte, *J. Paleontol.* **50**, 808 (1976).
5. K. Padian, in *The Beginning of the Age of Dinosaurs: Faunal Change Across the Triassic-Jurassic Boundary*, K. Padian, Ed. (Cambridge Univ. Press, New York, 1986), pp. 1–7.
6. M. J. Benton, *Modern Geol.* **13**, 41 (1988); H.-D. Sues, in (*2*), pp. 143–147.
7. A. P. Hunt and S. G. Lucas, *Palaeontology* **34**, 927 (1991); S. G. Lucas and A. P. Hunt, *Naturwissenschaften* **79**, 171 (1992).
8. M. J. Benton, *Nature* **321**, 857 (1986); in (*5*), pp. 303–320.
9. R. T. Bakker, *Evolution* **25**, 636 (1971); *The Dinosaur Heresies* (William Morrow, New York, 1986), pp. 75–101; A. J. Charig, in *Studies in Vertebrate Evolution*, K. A. Joysey and T. S. Kemp, Eds. (Oliver & Boyd, Edinburgh, United Kingdom, 1972), pp. 121–155; *Zool. Soc. London Symp.* **57**, 597 (1984).
10. M. A. Uliana, K. Y. Biddle, J. Cerdan, *Am. Assoc. Pet. Geol. Mem.* **46**, 599 (1989).
11. The paleoenvironment of the Ischigualasto Formation has been described as either a lush, lake-dominated setting characterized by a humid climate [P. L. Robinson, *Palaeontology* **14**, 131 (1971)] or a predominantly fluvial setting that experienced seasonal variations in water availability [G. E. Bossi, *Acta Geol. Lilloana* **4**, 75 (1970)]. The paleoclimatic indicators we recorded, such as paleovertisols, caliches, and the scarcity of freshwater vertebrates and invertebrates, are consistent with a seasonal, water-limited setting.
12. Valle de la Luna is the region in which nearly all previously described vertebrate fossils from the Ischigualasto Formation were discovered [A. S.

Romer, *Breviora* **156**, 1 (1962); O. Reig, *Ameghiniana* **3**, 3 (1963)].
13. D. J. Bottjer and D. Jablonski, *Palaios* **3**, 540 (1988).
14. M. J. Benton, *New Sci.* **7**, 9 (1983).
15. P. N. Stipanícic, in *The Phanerozoic Geology of the World: The Mesozoic*, M. Moullade and A. E. Nairn, Eds. (Elsevier, New York, 1983), vol. 2B, pp. 188–199. Relative-abundance data are needed for the pollen and macrofloral records to address fully this question.
16. J. F. Bonaparte, *J. Vertebr. Paleontol.* **2**, 362 (1982).
17. Percentages were calculated from a total sample of 238 specimens (228 specimens documented in Fig. 2 plus nine specimens mentioned in caption of Fig. 2 plus a single specimen of *Pisanosaurus*).
18. Tetrapod fossils typically occur as isolated skeletons or articulated skeletal components (limbs, vertebral segments, and skulls) in fine-grained overbank facies. Additional observations on the taphonomy of the Ischigualasto Formation can be found in R. R. Rogers *et al.*, *Fifth North Am. Paleontol. Conv. Abstr. Prog.* 249 (1992).
19. Analytical procedures follow (*28*) and references therein. The sanidine was treated with dilute (~0.7%) hydrofluoric acid for 5 min. to remove any altered glass and adhering clays and was then rinsed for 5 min. in distilled water. The sanidine was then irradiated together with a centrally located monitor mineral (Fish Canyon Tuff sanidine) for 14 hours in the Omega West research reactor at Los Alamos National Laboratory. After irradiation, single crystals of the monitor mineral and approximately 25 crystals of the Herr Toba sanidine were loaded into individual 2-mm-diameter wells of a copper sample disk and then placed within the sample chamber of the extraction system and baked out at 200°C for 8 hours. Incremental heating and total fusion of the samples and monitor mineral were accomplished with a 6-W coherent Ar-ion laser. The laser beam was not focused so that it would heat the sample wells evenly. Each well was also incrementally heated for 45 s by stepwise increases in the laser output. Purification of the released gases and data reduction are as in (*28*). The Ca and K corrections for this study, as determined from laboratory salts, are $(^{36}Ar/^{37}Ar)Ca = 2.582 \times 10^{-4} \pm 6.0 \times 10^{-6}$, $(^{39}Ar/^{37}Ar)Ca = 6.7 \times 10^{-4} \pm 3.0 \times 10^{-5}$, and $(^{40}Ar/^{39}Ar)K = 2.03 \times 10^{-2} \pm 4.0 \times 10^{-4}$. A value of 0.011294 ± 0.00001 for the fluence-calibration parameter J was based on eight replicate single-crystal analyses of the monitor mineral Fish Canyon sanidine with an age of 27.84 Ma. The age of the Fish Canyon sanidine adopted in this study is similar to that recommended by G. T. Cebula *et al.* [*Terra Cognita* **6**, 139 (1986)] but is slightly modified as a result of intercalibration with MMhb-I (Minnesota hornblende monitor mineral) with an age of 520.4 ± 1.7 Ma [S. D. Samson and E. C. Alexander, *Chem. Geol. Isot. Geosci. Sect.* **66**, 27 (1987)]. Mass discrimination during this study, as determined by replicate air aliquots delivered from an on-line pipette system, was 1.005 ± 0.002. Decay constants are those recommended by R. H. Steiger and E. Jäger [*Earth Planet. Sci. Lett.* **36**, 359 (1977)] and G. B. Dalrymple [*Geology* **7**, 558 (1979)].
20. Plateau definition basically follows R. J. Fleck *et al.*, *Geochim. Cosmochim. Acta* **41**, 15 (1977).
21. S. C. Forster and G. Warrington, in *The Chronology of the Geological Record*, N. J. Snelling, Ed. (Geological Society, London, 1985), pp. 99–113; J. W. Cowie and M. G. Bassett, *Episodes* **12** (no. 2), (suppl.) (1989); W. B. Harland *et al.*, *A Geologic Time Scale 1989* (Cambridge Univ. Press, New York, 1990).
22. A. G. Fischer, in *Cycles and Events in Stratigraphy*, G. Einsele, W. Ricken, A. Seilacher, Eds. (Springer-Verlag, New York, 1991), pp. 48–62; S. M. Kidwell, *Geol. Rundsch.*, in press. Sedimentation rates used are low to moderate for a rift basin setting.
23. P. E. Olsen and H.-D. Sues, in *The Beginning of the Age of Dinosaurs*, K. Padian, Ed. (Cambridge Univ. Press, New York, 1988), pp. 321–351.
24. Arguments for an end Carnian or late Carnian tetrapod extinction event are based on counts of families and species that have last appearances in the Tuvalian substage of the late Carnian [M. J. Benton, *Hist. Biol.* **5**, 263 (1991)]. Our data suggest that the Ischigualasto taxa *Trialestes*, *Ischigualastia*, *Scaphonyx*, *Exaeretodon*, *Pisanosaurus*, and *Proterochampsa*, until now placed in the latter half of the Tuvalian, are in fact older. Thus, our results diminish the apparent magnitude of the purported end Carnian extinction event by reducing the number of last appearance events known in the Tuvalian.
25. P. A. Murry and R. A. Long, in *Dawn of the Age of Dinosaurs in the American Southwest*, S. G. Lucas and A. P. Hunt, Eds. (New Mexico Museum of Natural History, Albuquerque, NM, 1989), pp. 29–64; J. M. Parrish, in *ibid.*, pp. 360–374.
26. By guild we imply a group of organisms that utilize a common resource in a similar fashion [R. B. Root, *Ecol. Monogr.* **37**, 317 (1967)]. No direct competition is implied.
27. P. C. Sereno, *J. Vertebr. Paleontol.* **11**, 168 (1991).
28. C. C. Swisher III *et al.*, *Science* **257**, 954 (1992).
29. Isolated skeletons or skeletal components were counted as one individual. If several fossils were found in close proximity on a single bedding plane, we determined the minimum number of individuals with methods reviewed in C. Badgley, *Palaios* **1**, 328 (1986).
30. W. D. Sill, *Mus. Comp. Zool. Bull.* **146**, 317 (1974).
31. The uncertainties associated with the individual incremental apparent ages are 2σ errors, whereas those that accompany the calculated weighted mean ages of the plateau increments and weighted means of the replicate analyses are standard errors (SE), following J. R. Taylor, *An Introduction to Error Analysis* (Oxford Univ. Press, New York, 1982).
32. We thank J. Alroy, M. Benton, D. Jablonski, T. Jordan, S. Kidwell, K. Roy, and N. Shubin for comments and suggestions and C. Abraczinskas for drafting the illustrations. We also thank all members of the joint Argentine-American field crews of 1988 and 1991 (O. Alcober, A. Arcucci, R. Gordillo, D. Herrera, C. May, F. Novas, W. Stevens, and C. Yu). Supported by grants from the David and Lucile Packard Foundation, the Petroleum Research Fund of the American Chemical Society, the National Geographic Society, the National Science Foundation (to P.C.S.), and the Institute of Human Origins (C.C.S.).

7 January 1993; accepted 29 March 1993

Copernicus: A Regional Probe of the Lunar Interior

Patrick C. Pinet, Serge D. Chevrel, Patrick Martin

Earth-based telescopic spectral imaging techniques were used to document the spatial distribution of crater materials within the large lunar crater Copernicus at the subkilometer scale on the basis of spectral ultraviolet–visible–near-infrared characteristics. The proposed spectral mixing analysis leads to a first-order mapping of the impact melt material within the crater. Olivine was detected not only within the three central peaks but also along a significant portion of the crater rim. Consideration of an olivine-bearing endmember in the mixing model emphasizes the overall morphological pattern of the rim and wall terraces in the associated fraction image. The identification of widely exposed olivine units supports the idea that the lower crust and possibly the lunar mantle itself are regionally at shallow depth.

Large impact craters such as Copernicus excavate materials from different depths and thus provide information at the target site on the preimpact stratigraphy and mineralogical heterogeneities of the lunar crust, both laterally and vertically (*1–3*). The recent Galileo lunar flyby revealed that the stratification of the lunar crust may be regionally affected by the presence of cryptomaria, especially on the western farside and nearside (*4*). However, the global multispectral information retrieved from the solid-state imaging (SSI) experiment onboard the Galileo spacecraft was limited in both spatial and spectral resolution, precluding any detailed geological analysis of morphological surface units such as impact craters. New Earth-based remote-sensing techniques have allowed powerful investigations of the nature and layering of the lunar crust by means of spectro-imaging analyses. In this report, we document the spatial distribution of crater materials within Copernicus at the subkilometer scale on the basis of their spectral ultraviolet (UV)–visible (VIS)–near-infrared (NIR) characteristics and compare these data with the results of previous spot-spectroscopic investigations (*1, 2, 5*).

We carried out an extensive Earth-based spectral mapping (UV-VIS-NIR domain) of Copernicus (93 km in diameter) with charge-coupled device (CCD) images that had high spatial (0.7 km) and spectral (wavelength/band pass = $\lambda/\Delta\lambda$ = 100) resolution. The observations were carried out in the September 1989 full-moon period, with a Thomson CCD camera mounted at the focus of the 2-m aperture (focal length/diameter = 25) telescope of the Pic-du-Midi Observatory (France) (*6, 7*), under 6° and 19° of phase angle, during two successive photometric nights (excellent atmospheric stability and less than 30% hygrometry). The optical configuration corresponds to a theoretical spatial sampling of 0.17 km per pixel at the subterrestrial point.

UPR 234/Centre National de la Recherche Scientifique, Groupe de Recherche en Geodésie Spatiale, Observatoire Midi-Pyrénées, Toulouse 31400, France.